

T_{eff} and $\log g$ dependence of FeH in M-dwarfs

S. Wende*, A. Reiners* and H.-G. Ludwig[†]

**Institut für Astrophysik, Georg-August-Universität Göttingen, Friedrich-Hund Platz 1, D-37077 Göttingen, Germany*

[†]GEPI, CIFIST, Observatoire de Paris-Meudon, 5 place Jules Janssen, 92195 Meudon Cedex, France

Abstract. We present synthetic FeH band spectra in the z -filter range for several M-dwarf models with $\log g = 3.0 - 5.0$ [cgs] and $T_{\text{eff}} = 2800 \text{ K} - 3450 \text{ K}$. Our aim is to characterize convective velocities in M-dwarfs and to give a rough estimate of the range in which 3D-atmosphere treatment is necessary and where 1D-atmosphere models suffice for the interpretation of molecular spectral features. This is also important in order to distinguish between the velocity-broadening and the rotational- or Zeeman-broadening. The synthetic spectra were calculated using 3D CO5BOLD radiative-hydrodynamic (RHD) models and the line synthesis code LINFOR3D. We used complete 3D-models and high resolution 3D spectral synthesis for the detailed study of some well isolated FeH lines. The FeH line strength shows a dependence on surface gravity and effective temperature and could be employed to measure both quantities in M-type objects. The line width is related to the velocity-field in the model stars, which depends strongly on surface gravity. Furthermore, we investigate the velocity-field in the 3D M-dwarf models together with the related micro- and macro-turbulent velocities in the 1D case. We also search for effects on the lineshapes.

Keywords: Radiative transfer - Line: profiles - Stars: atmospheres, low-mass, kinematics

PACS: 95.30.Jx, 95.30.Ky, 95.30.Lz, 95.75.Fg

SINGLE 3D- AND <3D>- FeH LINES

In this work, we use the radiative-hydrodynamic (RHD) model-atmospheres (see Tab. 1) which were computed with the CO5BOLD-code employing opacity binning (see e.g. [1] or [2]) with five bands to take into account the wavelength dependence of the radiative energy exchange. To calculate the spectral lines, we use the line synthesis code LINFOR3D¹, which is able to use the 3D capacity of the CO5BOLD-atmosphere models. We investigated 10 FeH lines between 9950 \AA and 9990 \AA which were chosen from [3] (see Tab. 2). The resolution of the synthetic spectra is $\Delta\lambda = 5 \cdot 10^{-3} \text{ \AA}$ corresponding to a Doppler velocity of $\approx 150 \text{ m/s}$ at the wavelength of the considered lines. We averaged over the spatial x-y directions in the 3D-model to receive a 1D-model, which we call the <3D>-model. This model is used for comparison between the modelled 3D and <3D> FeH lines to investigate the effect of micro and macro turbulent velocities. The 3D velocity fields are not taken into account in the <3D>-models, and line broadening is treated within the classical scheme of micro- and macro-turbulence. In Fig. 1 one can see that there is a strong influence of surface gravity and effective temperature on the lineshape for the 3D-models. Regarding the <3D>-models, the effect on line depth with

¹ see http://www.aip.de/~mst/Linfor3D/linfor_3D_manual.pdf

changing $\log g$ is less obvious. Line depth changes in the 3D case can be explained by line broadening by the hydrodynamical velocity field. The equivalent width of the lines is not strongly affected since they are only mildly saturated (see Fig. 2).

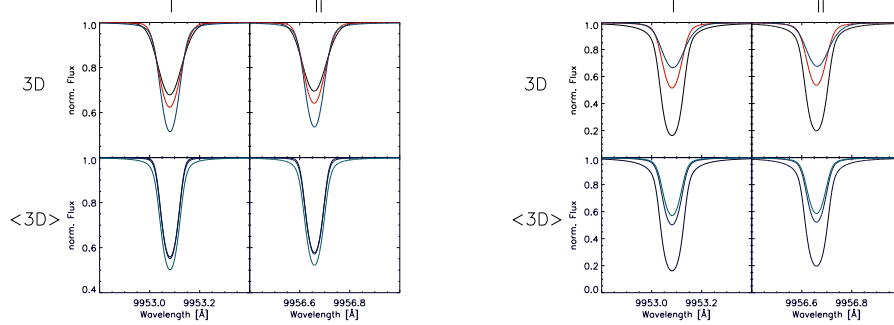


FIGURE 1. *Left:* Two out of ten simulated FeH lines (Tab. 2) for models with $T_{\text{eff}} = 3300\text{K}$ and $\log g$ values of 3.0, 4.0, and 5.0 [cgs]. The line centered at vacuum wavelength 9953.07 \AA is magnetically sensitive (label I) and the line centered at vacuum wavelength 9956.72 \AA is magnetically insensitive (label II). The upper panels show 3D lines with $\log g = 5.0$ (blue), 4.0 (red), and 3.0 (black) [cgs]. The lower panels show the same for the $\langle 3D \rangle$ lines. *Right:* The same as in the left plot for models with T_{eff} of 2800 K, 3300 K and 3450 K. All models have $\log g = 5.0$ [cgs]. The upper panels show 3D lines with $T_{\text{eff}} = 3450\text{ K}$ (blue), 3300 K (red), and 2800 K (black). The lower panels show the same for the $\langle 3D \rangle$ lines.

TABLE 1. Overview of different model quantities

Model code	Dim.	Size [km]	Opacities	T_{eff} [K]	$\log g$
d3t33g30mm00w1	3	85000 x 85000 x 58350	PHOENIX	3300	3.0
3dt3280g40mm00	3	4500 x 4500 x 1850	PHOENIX	3300	4.0
d3t33g50mm00w1	3	300 x 300 x 260	PHOENIX	3300	5.0
d3t35g50mm00w1	3	900 x 900 x 300	PHOENIX	3450	5.0
d3t28g50mm00w1	3	250 x 250 x 270	PHOENIX	2800	5.0

TABLE 2. Several quantities of the investigated FeH lines [3]. J is the angular momentum and Ω the ro-vibrational constant. Magn. sen. stands for magnetic sensitivity.

$\lambda_{\text{rest}}^{\text{air}}$ [Å]	Branch	J	ω	magn. sen.	$\lambda_{\text{rest}}^{\text{air}}$ [Å]	Branch	J	ω	magn. sen.
9950.34	R	10.5	1.5	no	9971.73	R	4.5	0.5	no
9951.27	P	16.5	2.5-3.5	yes	9975.48	Q	2.5	2.5	yes
9953.99	R	22.5	3.5	yes	9976.4	R	2.5	0.5	yes
9954.59	R	12.5	1.5	no	9978.72	R	6.5	0.5	no
9971.07	R	12.5	1.5	no	9979.87	Q	3.5	2.5	yes

To quantify the results visualized in Fig. 1, we measured the equivalent width, the gaussian FWHM, and the line depth of the ten investigated FeH-lines (see Tab. 2). A run of these quantities is plotted in Fig. 2.

Equivalent width (Fig. 2 top): The equivalent width shows little difference between the 3D and the $\langle 3D \rangle$ lines. This difference stays almost constant in both cases (different T_{eff} and $\log g$). This indicates that the deviations between the FeH lines are due to velocity broadening, which should only mildly affect the equivalent width. The run of the equivalent width in the $\log g$ -series seems to stay almost constant and is only weakly

dependent on surface gravity. With different effective temperatures the number of FeH molecules varies strongly and hence the equivalent width. It decreases with increasing T_{eff} due to the dissociation of the FeH-molecules.

Gaussian FWHM (Fig. 2 middle): The dependence of the line width (FWHM) on the surface gravity is very different for 3D- and <3D>-models. In the 3D case the FWHM decreases but in the <3D> case the FWHM increases with increasing surface gravity. The difference between 3D and <3D> lines at $\log g = 3.0$ is around 1 km/s. We point out that in the <3D>-model we did not add any micro- or macro-turbulence. The increasing line width in the 3D case is a consequence of the hydrodynamic velocity fields which increase strongly with decreasing $\log g$. In the T_{eff} series, the effect of velocity related broadening is not as strong as in the $\log g$ case, but we believe that the difference between 3D- and <3D>-models stems from the appearing velocity fields, too.

Line depth (Fig. 2 bottom): The difference in line depths between 3D- and <3D>-models is consistent with the velocity fields present in the atmospheres of the models. In the $\log g$ series the run of the line depth is very similar to the equivalent width and reflects the almost constant number of FeH molecules. In the T_{eff} series, the line depth shows a strong dependence on effective temperature and decreases with increasing T_{eff} .

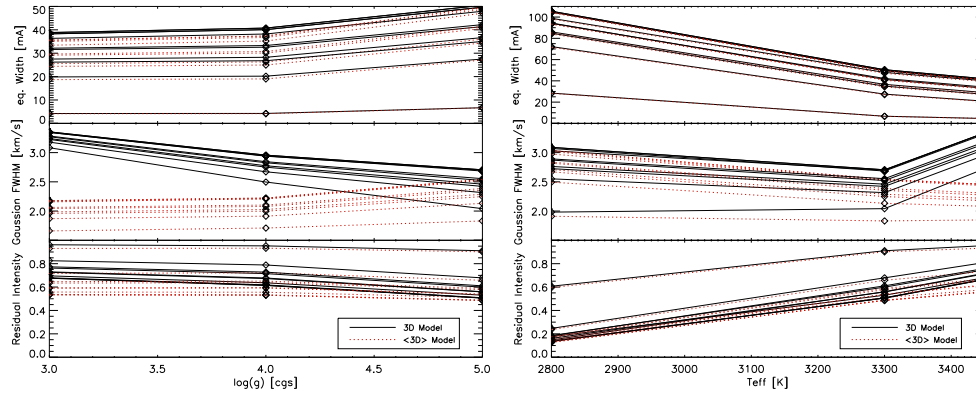


FIGURE 2. *Left:* Run of the equivalent width (top), the gaussian width (middle) and the line depth (bottom) for a model with $T_{\text{eff}} = 3300$ K and $\log g$ values of 3.0, 4.0 and 5.0 [cgs]. Plotted are the aforementioned quantities of the ten FeH-lines explained in Tab.2. For more information see text. *Right:* Same quantities and lines for T_{eff} 's of 2800 K, 3300 K and 3450 K and a $\log g$ value of 5.0 [cgs].

VELOCITY FIELDS

The velocity broadening has a noteworthy influence especially at low $\log g$ values. To investigate the velocity fields in the models, we use the *curve of growth* method. This employs the artificial increase of the line strength of a Ca I-line. Ca I-lines produced on <3D>-models with different micro-turbulent velocities enable us to determine a micro-turbulent velocity for the 3D-model. We use the Ca I micro-turbulent velocities to convolve the <3D>-model lines with gaussian velocity profiles. A comparison with <3D> lines which include the afore determined micro-turbulent velocities computed with LINFOR3D, shows that the difference between both lines is insignificant. We broaden these lines by convolution with a Gaussian profile again until they match the

3D lines and obtain an effective macro-turbulent velocity this way. The dependence of the micro- and macro-turbulent velocities on surface gravity and effective temperature is plotted in Fig. 3. One can see that the velocity field represents the behavior of the quantities investigated above and gives an explanation for the differences between 3D- and <3D>-models.

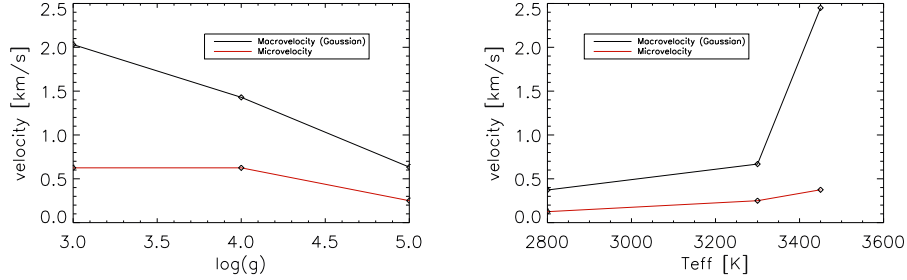


FIGURE 3. *Left:* Micro- and macro-turbulent velocities as a function of $\log g$. *Right:* Micro- and macro-turbulent velocities as a function of T_{eff} .

DISCUSSION

We have investigated ten single well isolated FeH lines between 9950 Å and 9990 Å on a set of 3D-CO5BOLD models, with the spectral synthesis code LINFOR3D. We found that the FeH lines react on different effective temperatures as one would expect due to the change in the FeH molecule number. The lines also show a weak dependence on surface gravity but if one includes the velocity-fields in the models, the $\log g$ dependence is strong due to the strong velocity broadening. This means for the 1D spectral synthesis that one has to include correct micro- and macro-turbulent velocities for small surface gravities or the line width would be too small up to 1 km/s. At high surface gravities, the FeH lines show a significant difference between <3D> and 3D models only for higher effective temperatures. This means that in the considered atmospheres thermal Doppler broadening is the dominant velocity-related broadening mechanism.

ACKNOWLEDGMENTS

SW would like to acknowledge the support from the DFG Research Training Group GrK - 1351 “Extrasolar Planets and their host stars”. AR acknowledges research funding from the DFG under an Emmy Noether Fellowship (RE 1664/4- 1). HGL acknowledges financial support from EU contract MEXT-CT-2004-014265 (CIFIST).

REFERENCES

1. H.-G. Ludwig, F. Allard, and P. H. Hauschildt, *A&A* **459**, 599–612 (2006).
2. H.-G. Ludwig, F. Allard, and P. H. Hauschildt, *A&A* **395**, 99–115 (2002).
3. A. Reiners, and G. Basri, *ApJ* **644**, 497–509 (2006).